Theor Chem Acc (2006) 115: 427–433
DOI 10.1007/s00214-006-0123-3

REGULAR ARTICLE

J.C. Sancho-García · A. Karpfen

Conformational analysis of 2,2′-bifuran: correlated high-level ab initio and DFT results

Received: 2 December 2005 / Accepted: 25 January 2006 / Published online: 22 February 2006

Abstract The torsional potential for inter-ring rotation in 2,2′-bifuran has been systematically tackled using highly accurate ab initio calculations as well as cost-effective DFT methods. The successful convergence of the ab initio results allowed to confirm the presence of a shallow gauche minimum in the torsional potential curve. The standard DFT methods failed to capture such a tiny energy barrier but, interestingly, the results could be remarkably improved by a mixture of wavefunction and DFT energies in a multi-coefficient fashion; thus, accurate DFT-based and ab initio reference data also become available. Since the experimental evaluation of torsional potentials faces quantitative problems, the outcome of high-level theoretical calculations is expected to be reliably used in further investigation on structure and conformational distribution of this system.

Keywords Conformational analysis · Torsional energy profiles · Ab initio calculations · Density-functional theory

PACS 31.15.Ar Ab initio calculations · 31.15.Ew Density-functional theory · 31.50.Bc Potential energy surfaces for ground electronic states · 33.15.Hp Barrier heights (internal rotation)

1 Introduction

The quantitative evaluation of torsional barrier heights of π-conjugated molecules needs well-rooted, cost-effective, although reliable, methods able to describe successfully the evolution of the electronic properties of these systems as a function of the torsional angle between adjacent rings. One of the main goals of contemporary computational chemistry is to achieve the so-called "chemical accuracy", which implies errors less than 1 kcal/mol, at moderate computational cost. For the calculation of torsional potentials this criterion is evidently insufficient. Since common barrier heights are usually of the same order of magnitude as $k_B T$, much more stringent conditions must be applied. For instance, it has been recently demonstrated that a pair of two competing processes, fluorescence or intermolecular electron transfer, in a perylenebisimide-based donor–acceptor molecule having a biphenyl derivative acting as donor critically depends on the torsional properties of the biphenyl core [1]. Another example is also provided by the influence of molecular conformations on the energetics of an organic/metal interface [2]. In this case, the injection energy barrier needed to initiate a charge transfer process is dictated by the non-rigidity of the molecule, *p*-sexiphenyl or *p*-sexithienyl, being physically adsorbed. A third situation is found in a recent computational study on the effect of confinement on the rotational isomerization of 1,3-butadiene [3]. The geometrical constraints imposed by the size of the nanopores, where the molecule is confined, critically affects the population of the conformers [4]. If closely related applications of furan-based oligomers [5–7] or polymers [8–10] are envisioned for the emerging but rapidly growing fields of nanolectronics and molecular devices, a thorough understanding and accurate modelling of torsional potentials along the whole range of dihedral angle needs to be achieved. Since most of the chemical phenomena involved in the operational mechanism of optoelectronic devices may be usually rationalized from the theoretical study of finite-size π-conjugated fragments [11], a systematic study of torsional potentials and energy barrier heights for inter-ring rotation in 2,2′-bifuran will be accomplished here. As experimental results are not available yet, the predictions of high-level calculations might provide a sound basis for further investigation on conformational equilibrium and associated properties. Although an interesting set of preliminary theoretical results is found in the literature [12–16], the question has not yet been addressed adequately due to the well-known computational bottleneck

J.C. Sancho-García (✉)
Departamento de Química Física,
Universidad de Alicante,
03080 Alicante, Spain
E-mail: JC.Sancho@ua.es

A. Karpfen
Institute for Theoretical Chemistry,
University of Vienna,
1090 Vienna, Austria
E-mail: Alfred.Karpfen@univie.ac.at

for highly accurate ab initio calculations. Additionally, after having established the desired benchmark results, density-functional theory (DFT) will be further applied due to its reduced computational cost. Despite being a cost-effective method, previous studies have shown several shortcomings of the most widely used exchange energy functionals in the description of torsion properties of π-conjugated molecules [17–19]. Therefore, the application of a large panel of exchange-correlation functionals in a systematic manner will also serve to address that feature along the work.

2 Methods and computational details

All calculations have been performed with the Gaussian 03 package [20]. Non-rigid calculations of torsional potentials require full optimization of the geometric structure of all conformers at the second-order Møller–Plesset theory (MP2) and DFT levels for each fixed value of the torsional angle ϕ. A regular grid was imposed for ϕ from 0° to 180° in steps of 10°. A set of benchmark coupled-cluster with single, double, and perturbatively estimated triple excitations, CCSD(T), single-point corrections were further performed using the former MP2 optimized geometries. The correlation-consistent (aug-)cc-pVnZ basis sets were applied due to their well-known large coverage of the one-particle space while keeping a good asymptotic behavior. The best-estimated value was thus obtained by adding the correction

$$\Delta\text{CCSD(T)} = \text{CCSD(T)/aug-cc-pVDZ//MP2/aug-cc-pVDZ} - \text{MP2/aug-cc-pVDZ} \quad (1)$$

to the MP2/cc-pVQZ//MP2/cc-pVTZ calculated energy. Sufficiently converged results were obtained at this level in close agreement with previous studies [21,22]; thus, the possible impact of further basis sets extension or higher levels of coupled-cluster theory is not expected to significantly influence the conclusions. Use of a higher-order level of perturbation theory in Eq. (1), MP4(SDTQ), instead of CCSD(T) did not appreciably modify the results. Other minor contributions such as core correlation effects, or scalar relativistic corrections, are not considered in the present work since their impact on the torsional barrier heights is expected to be negligible [23,24].

A general expression to systematically tune the mixing of exchange–correlation functionals with exact Hartree–Fock (HF) exchange (E_x^{HF}) may be defined as follows:

$$E_{xc}[\rho] = a_x E_x^{\text{HF}} + (1 - a_x)\, E_x[\rho] + E_c[\rho], \quad (2)$$

where $E_i[\rho]$ is one of the most employed exchange ($i{=}x$) or correlation ($i{=}c$) functionals. The coefficient a_x has been introduced to probe in a systematic way the influence of the exact exchange, which indeed primarily governs the torsional energy profiles of π-conjugated systems. We have selected two categories of density-functional methods, the Generalized Gradient Approximation (GGA) and the so-called m-GGA extension which includes new variables of the density in addition to its gradient $\nabla\rho(\mathbf{r})$. Among the former, the well-known B [25], mPW91 [26], or PBE [27] expressions were selected and, respectively, coupled to the LYP [28], PW91 [29], or PBE [27] correlation counter-parts. The hybrid versions resulting from the variation of a_x in Eq. (2) are termed B1LYP, mPW1, PBE0 ($a_x{=}0.25$) and BHHLYP, mPWHH, or PBEHH ($a_x{=}0.5$). The study further involves the compact expressions for the B97-1, B97-2, and B98 hybrid functionals, which are different reparameterizations of the B97 model [30]. PW91- [29] or B3LYP-based [31] results are also included since these functionals are often used as reference. The exchange–correlation m-GGA functionals included those based in the combination of OPTX exchange [32] and B95 correlation [33], as well as the recently developed TPSS model [34]. By analogy with previous standard procedures, the corresponding hybrid versions are named O1B95 (TPSS0) and OHHB95 (TPSSHH). Note that empirical mixing of TPSS with exact HF exchange is also allowed (TPSSh, $a_x{=}0.1$ [35]) without violating the exact constraints which precisely define the model. Previously reported results were only obtained at the B(3)LYP level. The present study broadly expands the set of applied exchange–correlation functionals and thus the assessment of the theory. All the DFT results were obtained with the cc-pVTZ basis sets, which ensure a large coverage of the one-particle space. As a matter of fact, the inclusion of diffuse functions (aug-cc-pVTZ) or an additional set of polarization functions (cc-pVQZ) only marginally affected the results, a set of test calculations were done at the BHHLYP level, and thus the results are not expected to significantly vary upon further basis sets extension.

3 Results and discussion

3.1 Benchmark ab initio calculations

The torsional potential of 2,2′-bifuran shows an energy profile remarkably different from other heteroaromatic dimers as 2,2′-bipyrrole [22] or 2,2′-bithiophene [13,36]. We would like to particularly emphasize the absence of the *anti*-gauche conformer and the minute energy difference between the *syn* and *syn*-gauche forms. Furthermore, in view of the non-conclusive results existing up to date about these features, large-scale ab initio calculations need to be pursued in order to extend previous studies [15]. We have thus collected in Table 1 the MP2-calculated barrier heights employing the set of (aug-)cc-pVnZ basis functions. The corresponding torsional curves are shown in Fig. 1. Whereas the MP2 results may be considered as virtually converged at the cc-pVQZ level, the convergence of the correlation energy needs to be further explored beyond the MP2 truncation. To do so, approximate CCSD(T) results were constructed by adding the energy difference between CCSD(T)/aug-cc-pVDZ//MP2/aug-cc-pVDZ and MP2/aug-cc-pVDZ to the MP2 energies obtained with the largest basis. The last entry of Table 1 reports the best-estimated value, named MP2/cc-pVQZ + ΔCCSD(T), which will be used in the next sections as

Table 1 Energetics (kcal/mol) of stationary points in 2,2′-bifuran relative to the *anti*-planar conformation, as calculated at the MP2 level with different basis sets, with the corresponding angle (in degrees) in parentheses

Method	TS-*syn-anti*	*syn*-Gauche	*syn*
MP2/cc-pVDZ	3.81 (93.9°)	1.78 (15.3°)	1.80 (0°)
MP2/aug-cc-pVDZ	2.98 (97.3°)	1.36 (28.7°)	1.49 (0°)
MP2/cc-pVTZ	3.71 (94.6°)	1.52 (17.9°)	1.54 (0°)
MP2/aug-cc-pVTZ[a]	3.56 (94.6°)	1.46 (19.3°)	1.51 (0°)
MP2/cc-pVQZ[a]	3.63 (94.6°)	1.47 (15.3°)	1.49 (0°)
MP2/cc-pVQZ[a] + ΔCCSD(T)	3.92 (96.1°)	1.71 (20.3°)	1.76 (0°)

[a] At the corresponding MP2/cc-pVTZ optimized geometry

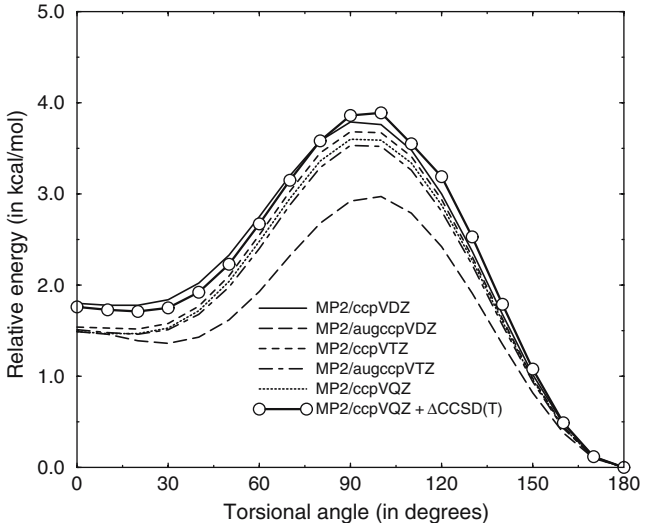

Fig. 1 Torsional potential of 2,2′-bifuran, as calculated at the MP2 level with different basis sets

reference. As it is easily seen a very shallow *syn*-gauche minimum is consistently found at all levels of theory. However, an energy barrier well below 0.1 kcal/mol will not sustain a vibrationally stable state thus giving rise to more pronounced large amplitude motions around the *syn* structure. As a result, since experimental information is still not available, a mixture of both conformers, *syn* and *anti*, is predicted.

3.2 Application of exchange–correlation functionals

The performance of the large set of assessed exchange–correlation functionals is shown in Table 2. Figures 2 and 3 display the torsional potential for a set of representative GGA and m-GGA results, respectively. The analysis of the results allows us to conclude that: (1) all the DFT methods show an amazingly narrow range of values for the energy barriers, deviations of 0.5 kcal/mol at most between a pair of randomly selected functionals, independent of the exchange–correlation kernel being used; (2) it might be argued that recently developed m-GGA functionals provide slight improvements with respect to former and well-established functionals, B3LYP being often taken as reference, but major breakthroughs are not achieved; (3) whereas all the DFT methods are able to provide rather accurate values for the *anti*/*syn* energy separation, none of them (except OB95) fulfills the "calibration accuracy" required for the barrier needed to reach the highly twisted TS-*syn-anti* form; (4) a larger percentage of HF exchange helps the *anti*/*syn* barrier to converge towards the reference value but, contrarily to what is observed in other systems [22], progressively deteriorates the results in the 30°–150° range; (5) the recently devised, and closely related, B97-1, B97-2, and B98 schemes behave almost similarly in the calculation of torsional potentials, as is actually expected [19] for highly parameterized specific-purposes functionals that operate out of their fitting range. However, in spite of the aforesaid features, the most striking conclusion seems to be the general inability shown by all the hybrid and non-hybrid functionals to predict the shallow minimum for the *syn*-gauche structure.

3.3 Analysis using an aromaticity criterion

As the DFT-based molecular geometries are readily accessible along the torsional path, we have characterized next the extent of electronic π-delocalization by referring to the Harmonic Oscillator Model of Aromaticity (HOMA), undoubtedly one of the most utilized indices along the last years, defined as [37]

$$\mathrm{HOMA} = 1 - \frac{\alpha}{m}\sum_i \left(r_{\mathrm{opt}} - r_i\right)^2, \qquad (3)$$

where r_i is the length of the ith bond between non-hydrogen atoms out of the m involved in the summation; α an empirical constant fixed to give HOMA=0 for a model non-aromatic system, and HOMA=1 for a systems with all the bond lengths equalized to the optimal value r_{opt}. The HOMA index has become a very effective way to quantify the degree of π-delocalization over a conjugated fragment [38]. It is applied here to rationalize from a new perspective one of the main shortcomings arising from the application of DFT to the problem of torsion, i.e., the over-estimation of the energy barriers between the planar (fully delocalized) and non-planar (delocalization severely missed) structures. We represent in Fig. 4 the evolution of the normalized quantity HOMA(ϕ) − HOMA (180°) as a function of the dihedral angle for a couple of representative functionals, PBE- and OB95-based models. The conclusions are, however, completely independent of the functional studied and thus apply to the large set of models employed here. Such a selected input reflects the variation

Table 2 Energetics (kcal/mol) of stationary points in 2,2′-bifuran relative to the *anti*-planar conformation, as calculated at various DFT levels with the cc-pVTZ basis sets, with the corresponding angle (in degrees) in parentheses

Method		a_x	TS-*syn*-*anti*	*syn*-Gauche	*syn*
$E_{xc}^{GGA}[\rho]$	PW91	0	5.27 (93.5°)	–	1.48 (0°)
and	mPW91	0	5.14 (93.2°)	–	1.46 (0°)
hybrid	mPW1	0.25	5.22 (94.2°)	–	1.62 (0°)
versions	mPWHH	0.50	5.33 (95.3°)	–	1.78 (0°)
	PBE	0	5.21 (93.3°)	–	1.46 (0°)
	PBE0	0.25	5.26 (94.3°)	–	1.61 (0°)
	PBEHH	0.50	5.36 (95.3°)	–	1.77 (0°)
	BLYP	0	5.04 (93.4°)	–	1.58 (0°)
	B3LYP	0.20	5.18 (94.3°)	–	1.71 (0°)
	B1LYP	0.25	5.17 (94.4°)	–	1.75 (0°)
	BHHLYP	0.50	5.34 (95.3°)	–	1.94 (0°)
	B97-1	0.21	5.21 (94.2°)	–	1.62 (0°)
	B97-2	0.21	5.17 (94.2°)	–	1.58 (0°)
	B98	0.22	5.20 (94.2°)	–	1.64 (0°)
$E_{xc}^{m-GGA}[\rho]$	OB95	0	4.88 (93.3°)	–	1.31 (0°)
and	O1B95	0.25	5.00 (94.3°)	–	1.49 (0°)
hybrid	OHHB95	0.50	5.19 (95.4°)	–	1.68 (0°)
versions	TPSS	0	5.32 (93.3°)	–	1.48 (0°)
	TPSSh	0.10	5.32 (93.7°)	–	1.55 (0°)
	TPSS0	0.25	5.35 (94.3°)	–	1.64 (0°)
	TPSSHH	0.50	5.43 (95.3°)	–	1.79 (0°)
MP2/cc-pVQZ[a] + ΔCCSD(T)			3.92 (96.1°)	1.71 (20.3°)	1.76 (0°)

[a] At the corresponding MP2/cc-pVTZ optimized geometry

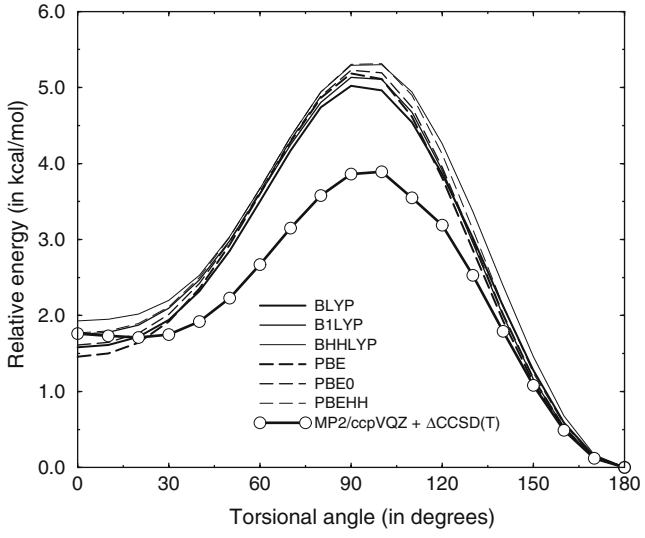

Fig. 2 Torsional potential of 2,2′-bifuran, as calculated at various GGA levels with the cc-pVTZ basis

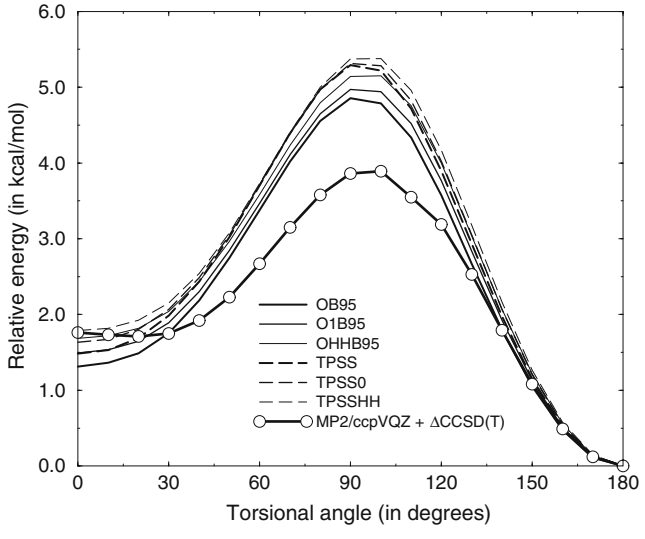

Fig. 3 Torsional potential of 2,2′-bifuran, as calculated at various m-GGA levels with the cc-pVTZ basis

of the degree of π-delocalization with respect to the value for the most stable conformer. The most accurate available results (MP2/cc-pVTZ) are taken as reference. Although non-bonding effects are known to play a key role in the regions around the planar conformers, the effective overlap of the curves is only produced in the 0°–30° and 150°–180° regions, which indeed should contribute to the accurate *anti*/*syn* barriers predicted by all the DFT methods. On the other hand, the PBE or OB95 functionals clearly over-estimate the difference HOMA(ϕ) − HOMA(180°) in the 30°–150° range of angles. This feature directly translates to the over-estimation of the difference between the strength of the π-conjugation of the planar and highly twisted forms, which may be traced back to the inadequacies of current exchange functionals to accurately describe the fully delocalized forms [17–19]. Additionally, the progressive incorporation of HF exchange slightly increases such difference and thus the corresponding TS-*syn*-*anti*/*anti* barrier height, as is the fact observed in Table 2.

Table 3 MC3-calculated energetics (kcal/mol) of stationary points in 2,2′-bifuran relative to the *anti*-planar conformation; results from its individual components are also listed and the corresponding angle (in degrees) is reported in parentheses

Method	TS-*syn*-*anti*	*syn*-Gauche	*syn*
HF/DIDZ	5.05 (97.4°)	2.36 (18.0°)	2.38 (0°)
MP2/DIDZ	2.02 (94.8°)	1.01 (37.3°)	1.85 (0°)
MPWX/MG3S	5.12 (94.9°)	–	1.67 (0°)
MC3MPWX	4.02 (94.6°)	1.54 (16.5°)	1.67 (0°)
BBX/MG3S	5.08 (95.2°)	–	1.64 (0°)
MC3BBX	4.24 (94.9°)	1.57 (13.4°)	1.65 (0°)
MP2/cc-pVQZ[a] + ΔCCSD(T)	3.92 (96.1°)	1.71 (20.3°)	1.76 (0°)

[a] At the corresponding MP2/cc-pVTZ optimized geometry

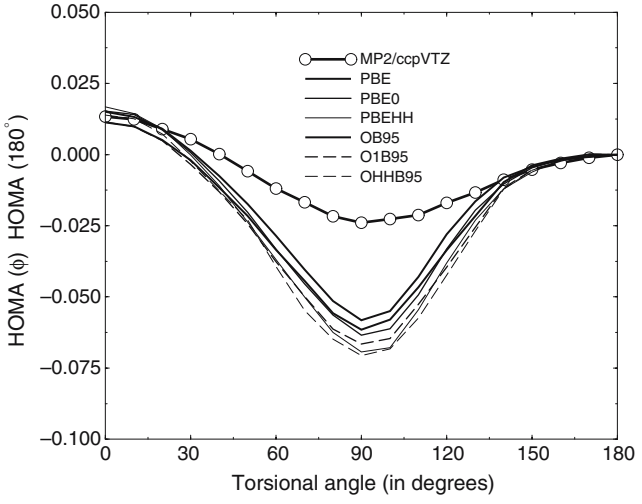

Fig. 4 Evolution of the HOMA index along the torsion, as calculated at various DFT levels with the cc-pVTZ basis

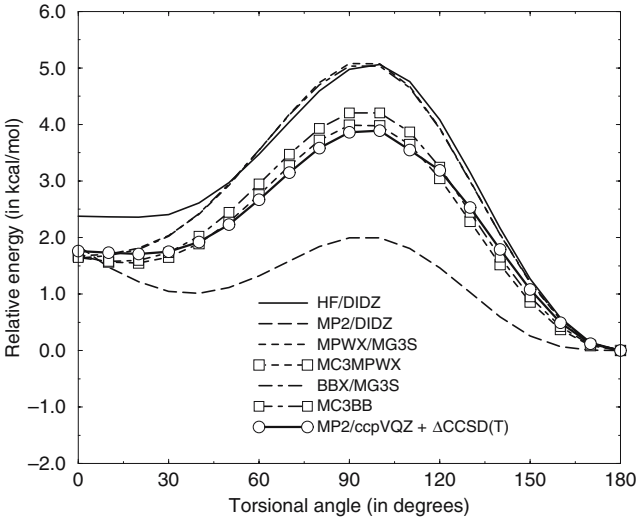

Fig. 5 Torsional potential of 2,2′-bifuran, as calculated by MC3-based approaches

3.4 Multicoefficient strategies

Multicoefficient (MC) protocols have been recently launched as a new suite of appealing computational tools; DFT schemes are actually combined with HF and MP2 methods in a three-parameter (MC3) version [39]

$$E_{\mathrm{MC3F}} = c_2\left[E_{\mathrm{HF/DIDZ}} + c_1\left(E_{\mathrm{MP2/DIDZ}} - E_{\mathrm{HF/DIDZ}}\right)\right] + (1 - c_2)\, E_{\mathrm{F}[\rho]/\mathrm{MG3S}}, \quad (4)$$

where F[ρ] is the density functional being employed, *i.e.*, either the MPWX (MC3MPWX) or the BBX (MC3BBX) exchange–correlation functional. Note that these two functionals are slightly modified versions, the percentage of HF exchange is reparameterized, compared to the MPW1k [40] and the BB1k [41] models. The pair of parameters (c_1, c_2) entering into Eq. (4) are easily extracted from the original reference. Note also that the higher computational cost of the MC3-based methods (N^5) compared to the formal cost of a DFT calculation (N^4) is, however, reduced due to the use of a specially suited basis sets (DIDZ) for the ab initio part. The DIDZ and MG3S basis sets correspond, in standard notation, to 6-31+G(d,p) and 6-311+G(2df,2p). These methods have recently provided remarkable accuracy when dealing with torsional energy profiles of π-conjugated molecules [22,42]; thus, the inclusion here can be considered as further attempt to confirm their reliability in the prediction of accurate torsional potentials of heteroaromatic dimers.

The performance of these MC3-based approaches is shown in Table 3, where the relative energies and torsional angles are reported and in Fig. 5, where the respective torsional curves are compared to the previously obtained reference data. Interestingly enough all the calculated barrier heights are in the "chemical accuracy" range; furthermore, even the most stringent "calibration accuracy" criterion (error less than ±1 kJ/mol) is achieved in most cases. As the results from their separate components are also included, it seems that the small DIDZ basis set is not able to accurately capture the major effects if used separately at the HF or MP2 level. As expected, the MG3S extension does not lead to very accurate results in combination with functionals including a large portion of HF exchange (MPWX, 38%; BBX, 39%). In summary, partly due to the compensation of two opposite trends (over-estimation and under-estimation of barrier heights by HF and MP2 methods, respectively) the customized combination in a three-parameter fashion of HF/DIDZ, MP2/DIDZ, and MPWX/MG3S or BBX/MG3S energies clearly outperforms the previous DFT results.

Table 4 Fitted expansion coefficients (kcal/mol) for the analytical torsional potential of 2,2′-bifuran

Method	V_1	V_2	V_3	V_4	V_5	V_6	V_7	V_8
MP2/cc-pVQZ[a] + ΔCCSD(T)	0.812	2.980	0.912	−0.248	0.048	−0.002	−0.014	−0.030
MC3MPWX	0.902	3.219	0.730	−0.419	−0.031	−0.044	0.037	−0.026
MC3BBX	0.893	3.441	0.730	−0.378	−0.044	−0.040	0.042	−0.017

[a] At the corresponding MP2/cc-pVTZ optimized geometry

3.5 Analytical Fourier fits

The most accurate point-wise calculated energies were subsequently used to obtain the corresponding Fourier expansion of the torsional potentials according to the form

$$V(\phi) = \sum_{n=1}^{m} V_n \left[1 - \cos n\,(180 - \phi)\right], \qquad (5)$$

where V_n are the coefficients to be fitted and ϕ the inter-ring torsional angle. Such a potential energy function is almost universally included in all current force fields and, consequently, it is of much interest to determine these expansion coefficients as accurate as possible. Fits extended here up to the eight order yield a sufficiently negligible difference between calculated and fitted values. The corresponding results for the best-behaved methods tested in this work are gathered in Table 4.

4 Concluding remarks

The torsional potential in 2,2′-bifuran has been studied in great detail using a large number of quantum-mechanical methods. Unprecedentedly accurate results were obtained by a combination of ab initio MP2 and CCSD(T) methods with the one-particle space expanded up to the cc-pVQZ level, thus making available a very precise Fourier series expansion of the torsional curve. The global minimum is the *anti*-planar conformer, whereas the second minimum corresponds to the *syn*-gauche structure and its symmetrical equivalent. These, together with the *syn* saddle point, form a symmetrical double minimum potential which is, however, not sufficiently deep to sustain a vibrational state. Therefore, the vibrationally averaged structure of the second most stable conformer will effectively have the planar *syn* structure. In agreement with previous theoretical studies the energy difference between the *anti* and *syn* conformers is less than 2 kcal/mol. At experimental conditions the presence of both isomers as well as the interconversion between the two conformers has to be expected. None of the broad set of standard density functionals agreed with the qualitative shape of the torsional potential around the *syn* structure, as obtained from high-level ab initio studies. In fact, the second most stable structure was predicted to be *syn*-planar conformer. The consequence of the inability of the applied DFT approaches to describe the shallow *syn*-gauche minimum is a considerably narrower potential around the *syn* structure, which leads to the well-known tendency of exchange energy functionals to over-estimate the relative energies of the twisted forms. A cost-effective path to systematically improve the results, based on a combination of DFT and wave function energies, has finally allowed to overcome these flaws and thus merge the two categories of methods.

Acknowledgements The work in Alicante is supported by the "Ministerio de Educación y Ciencia" of Spain and the "European Regional Development Fund" through project CTQ2004-06519/BQU; the regular grants of the "Vicerrectorado de Investigación" of the University of Alicante (VIGROB2005-96) are also acknowledged. JCSG also thanks the "Ministerio de Educación y Ciencia" of Spain for a research contract under the "Ramón y Cajal" program and the "Generalitat Valenciana" for economic support. The ab initio calculations were performed at the Linux-cluster Schrödinger III of the University of Vienna. The authors are grateful for ample supply of computer time on these installations.

References

1. Holman MW, Yan P, Ching K-C, Liu R, Ishak FI, Adams DM (2005) Chem Phys Lett 413:501
2. Koch N, Heimel G, Wu J, Zojer E, Johnson RL, Brédas J-L, Müllen K, Rabe JP (2005) Chem Phys Lett 413:390
3. Santiso EE, George AM, Sliwinska-Bartkowiak M, Nardelli MB, Gubbins KE (2005) Adsorption 11:349
4. Kofranek M, Karpfen A, Lischka H (1992) Chem Phys Lett 189:281
5. Ma J, Li S, Jiang Y (2002) Macromolecules 35:1109
6. Miyata Y, Nishinaga T, Komatsu K (2004) J Org Chem 70:1147
7. Wang Y, Ma J, Jiang Y (2005) J Phys Chem A 109:7197
8. Salzner U, Lagowski JB, Pickup PG, Poirier RA (1998) Synth Met 96:177
9. Ivanov I, Gherman BF, Yaron D (2001) Synth Met 116:111
10. Hutchison GR, Zhao Y-J, Delley B, Freeman AJ, Ratner MA, Marks TJ (2003) Phys Rev B 68:035204
11. Brédas JL, Beljonne D, Coropceanu V, Cornil J (2004) Chem Rev 104:4971
12. Ortí E, Sánchez-Marín J, Merchán M, Tomás F (1987) J Phys Chem 91:545
13. Karpfen A, Choi CH, Kertesz M (1997) J Phys Chem A 101:7426
14. Balbás A, González-Tejera MJ, Tortajada J (2001) J Mol Struct (Theochem) 572:141
15. Duarte HA, Duani H, De Almeida WB (2003) Chem Phys Lett 369:114
16. Liu F, Zuo P, Meng L, Zheng S (2005) J Mol Struct (Theochem) 726:189
17. Sancho-García JC, Pérez-Jiménez AJ, Moscardó F (2001) J Phys Chem A 105:10541
18. Sancho-García JC, Brédas JL, Cornil J (2003) Chem Phys Lett 377:63
19. Sancho-García JC, Cornil J (2004) J Chem Phys 121:3096
20. Frisch MJ et al (2003) GAUSSIAN03 revision C.02. Gaussian, Inc., Pittsburgh
21. Karpfen A, Parasuk V (2004) Mol Phys 102:819
22. Sancho-García JC, Karpfen A (2005) Chem Phys Lett 411:321
23. Császár AG, Szalay V, Senent ML (2004) J Chem Phys 120:1203

24. Pérez-Jiménez AJ, Pérez-Jordá JM, Sancho-García JC (2005) J Chem Phys 123:134309
25. Becke AD (1988) Phys Rev A 38:3098
26. Adamo C, Barone V (1998) J Chem Phys 108:664
27. Perdew JP, Burke K, Ernzerhof M (1996) Phys Rev Lett 77: 3865
28. Lee C, Yand W, Parr RG (1988) Phys Rev B 37:785
29. Perdew JP (1992) In: Ziesche P, Eschig H (eds) Electronic structure of solids'91. Akademie Verlag, Berlin, p 11
30. Becke AD (1997) J Chem Phys 107:8554
31. Becke AD (1993) J Chem Phys 98:5648
32. Handy NC, Cohen AJ (2001) Mol Phys 99:403
33. Becke AD (1996) J Chem Phys 104:1040
34. Perdew JP, Tao J, Staroverov VN, Scuseria GE (2004) J Chem Phys 120:6898
35. Staroverov VN, Scuseria GE, Tao J, Perdew JP (2003) J Chem Phys 119:12129
36. Raos G, Famulari A, Marconi V (2003) Chem Phys Lett 379:364
37. Krygowski TM, Cyrañanski MK (2001) Chem Rev 101:1385
38. Cyrañanski MK, Krygowski TM, Katritzky AR, Schleyer PVR (2002) J Org Chem 67:1333
39. Zhao Y, Lynch BJ, Truhlar DG (2004) J Phys Chem A 108:4786
40. Lynch BJ, Fast PL, Harris M, Truhlar DG (2000) J Phys Chem A 104:4811
41. Zhao Y, Lynch BJ, Truhlar DG (2004) J Phys Chem A 108:2715
42. Sancho-García JC (2005) J Phys Chem A 109:3470